

Advancing Data for Street-Level Flood Vulnerability: Evaluation of Variables Extracted from Google Street View in Quito, Ecuador

RAYCHELL VELEZ¹, DIANA CALDERON¹, LAUREN CAREY¹, CHRISTOPHER AIME¹, CAROLYNNE HULTQUIST^{1,2},
GREG YETMAN², ANDREW KRUCZKIEWICZ^{1,3}, YURI GOROKHOVICH¹, AND ROBERT S. CHEN^{1,2}

¹City University of New York, Lehman College, New York, NY 10468 USA

²Center for International Earth Science Information Network, Columbia Climate School, Columbia University, Palisades, NY 10964 USA

³International Research Institute for Climate and Society, Columbia Climate School, Columbia University, Palisades, NY 10964 USA

CORRESPONDING AUTHOR: CAROLYNNE HULTQUIST (e-mail: c.hultquist@columbia.edu)

This work was supported in part by NASA Goddard Space Flight Center under Grant 80GSFC18C0111 and in part by the Continued Development and Operation of Socioeconomic Data and Applications Center as a Distributed Archive Center, led by the Center for International Earth Science Information Network at Columbia University, and NASA under Grant 80NSSC18K0342.

This article has supplementary downloadable material available at <https://doi.org/10.1109/OJCS.2022.3166887>, provided by the authors.

ABSTRACT Data relevant to flood vulnerability is minimal and infrequently collected, if at all, for much of the world. This makes it difficult to highlight areas for humanitarian aid, monitor changes, and support communities in need. It is time consuming and resource intensive to do an exhaustive study for multiple flood relevant vulnerability variables using a field survey. We use a mixed methods approach to develop a survey on variables of interest and utilize an open-source crowdsourcing technique to remotely collect data with a human-machine interface using high-resolution satellite images and Google Street View. Finally, we perform an inter-rater agreement to assess if this technique provides consistent results. This paper focuses on Quito, Ecuador as a case study, but the methodology can be replicated to produce labeled training data in other areas. The overall goal is to advance methods to help build training datasets that allow for assessing and automating the mapping of flood vulnerability for urban areas.

INDEX TERMS Buildings, crowdsource, data collection, hazard, infrastructure, vulnerability.

I. INTRODUCTION

Flood risk occurs at the intersection of hydrologic conditions and exposure, with vulnerability indicating the propensity for loss. Urban flood vulnerability is multidimensional and encompasses many aspects such as physical, socioeconomic, and institutional [1]. Understanding the drivers of flood vulnerability in cities is crucial as globally urban populations continue to grow rapidly. In 2018, 55% of the world's population lived in urban areas and by 2050 the urban share of the global population is projected at 68% [2]. Floods are specifically exacerbated by urban environments where limited surface water infiltration and poorly maintained drainage systems increase risk [3]–[5].

Flood vulnerability assessment methods range in complexity and approach. Researchers have used regression methods to quantify the contribution of possible explanatory parameters to aspects of flood impact such as damage [6], probability to suffer flooding [7], or inundation frequency [8]. Multicriteria GIS methods combine several different standardized factors, often weighted by relative importance, using sets of rule-based algorithms to determine areas of flood vulnerability [9]. Some flood models are based solely on hydrologic and hydraulic parameters [10]. Integrated and multiple vulnerability assessments examine multiple domains of vulnerability such as physical, ecological, technological, and social [11]–[13]. Vulnerability curves relate the intensity of a process (e.g., water depth, velocity, or flood duration) to the corresponding degree of loss [14]–[16]. Many different

flood vulnerability indices exist, which combine a set of standardized indicators to produce an overall vulnerability score [17], [18]. Data Envelopment Analysis (DEA) has been used to obtain a flood social vulnerability index to which further statistical analysis could be applied [19].

Regardless of specific analytical tools, all the above methods are heavily dependent on data availability, accessibility, and quality, which is often poor in highly vulnerable areas. Moreover, data can be incomplete and/or inconsistent [20] or not available at all. Therefore, alternative crowdsourcing methods can be used to provide fast, easy, and cheap data collection. The reliability of crowdsourced collection techniques can be assessed through statistical methods such as inter-rater agreement and intraclass correlation agreement used to assess quality, integrity, and reproducibility. We present this study as a data driven analytic approach to bridge a mechanical turking method with the development of training data that can be used in damage modeling or machine learning based flood vulnerability analysis.

Ecuador is a country with diverse terrain with coastal, mountain, and rainforest regions. Approximately 9 million inhabitants of Ecuador live in urban areas, with 96% of these populations living in coastal and mountainous regions [21]. The most densely populated areas of Ecuador are also where significant risk of natural hazards exists, including the largest metropolitan areas of Quito and Guayaquil [21]. We select the city of Quito, Ecuador as a case study to test out our methodology. Quito is a high-altitude urban environment with 2 million people situated in mountains and valleys surrounded by steep terrain. Many people are exposed to flooding, however the level of exposure varies considerably due to both geophysical and socioeconomic factors [22]. The concentration and growth of population in urban areas increase the level of exposure to adverse natural events, in particular the evolution of the informal settlement areas [23], [24]. Quito is situated in a watershed basin in a mountainous area that is highly vulnerable to flooding, especially flooding that is triggered by heavy rainfall events [25]. The combination of small catchments with large areas of impervious surfaces and short flow concentration timing causes rivers to rapidly overflow into the built environment and for drainage systems to collapse [26]. This causes severe damage to civil infrastructure, housing, and agriculture, health impacts and disruption to communication and other systems.

In this study, we design a survey and develop a Mechanical Turking approach to capture street-level variables associated with flood vulnerability from Google Street View (GSV) and satellite imagery [27], [28]. A team of researchers with GIS experience were tasked with selecting appropriate variables to collect, building a consistent dataset by development of a standardized codebook and evaluation, and conducting the data collection through the local Mechanical Turk (MTurk) interface [29]. The constructed dataset will provide the training data for a machine learning model to estimate flood vulnerability in urban areas.

GSV is a feature within Google mapping products which allows users to interact with panoramic views of the Earth's surface [27]. Google collects street images using panoramic cameras, and in addition, displays images that are contributed by the public. Initially released in May 2007 for five U.S. cities, GSV included Quito in November 2015 and has continued to update imagery as of 2021 [30], [31]. By 2019, GSV had reached more than 10 million miles of global street coverage [32], [33]. A study on GSV in Latin American cities found GSV available about half the time within 100m of the 2019 OpenStreetMap (OSM) road layer [34].

Early studies of virtual audit tools using GSV confirmed reliability in relation to physical audits [35], [36] and demonstrated the use of remote sensing alongside GSV [37]. Sampling approaches have been developed to ensure that neighborhoods of different socioeconomic characteristics are represented [38]. Another study on neighborhood conditions found agreement across raters through their GSV linked web-application as a cost-effective virtual audit tool [39]. Virtual audits have assessed the performance of collection at one point of view instead of along a road segment [40] and the potential for longitudinal studies [41].

There is a growing body of research acknowledging GSV as a component of flood vulnerability assessment. GSV has been used to collect physical building characteristics that contribute to flood vulnerability based on visual inspection of the imagery [7], [15], [42], [43]. Collection methods range from visual inspection by a user, to deep learning methods trained to pick out specific features in the images. For example, using a neural network to detect doors from GSV images, estimate the doors' 3D coordinates relative to the camera's center, and automatically calculate the elevation of the door bottom edge [44]. Building footprints derived from inspection of satellite imagery and cadastral data have been cross-checked against GSV imagery to fill gaps in or validate data [6]. One study found a high reliability of using GSV to assess physical vulnerability when compared to ground control points from a field survey [42]. Validation of GSV data collected in flood vulnerability research is relatively uncommon.

Physical building characteristics acquired through GSV can be used as variable inputs for regression [7], vulnerability curves [15], as well as for flood loss estimation models [43]. The use of GSV in combination with available local building data may improve accuracy of physical building characteristic inventories. A study by Mostafiz *et al.* [43] suggested that data collected from GSV, combined with a local county-level building inventory, and the 2019 National Building Cost Manual, enhanced estimates for building attribute variables, particularly building replacement cost and foundation height. These improvements when compared to attribute data in the National Structure Inventory (NSI) 2.0 potentially contributed to better flood loss estimation accuracy [43].

II. METHODS AND PROCEDURES

We utilize a free, open-source local computer version of Mechanical Turk (MTurk) [45] as a platform to collect variables

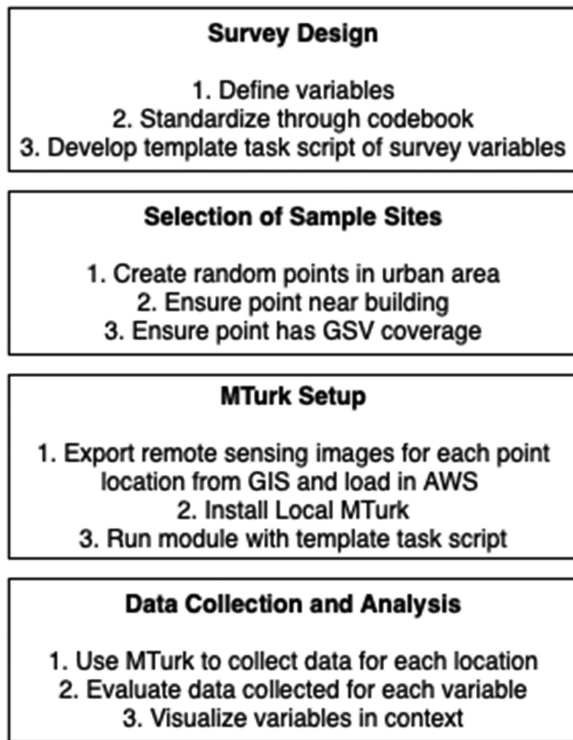


FIGURE 1. Flowchart of the methodology from survey design and site selection to the MTurk setup for data collection and the analysis of variables.

by expert GIS researchers in our team. An interface using the MTurk environment was implemented with two primary inputs: 1) a survey document that includes our variables of interest for collection, and 2) geographic coordinates associated with remote sensing imagery and GSV. Fig. 1 outlines our methodological process and corresponds to the following sections.

A. SURVEY DESIGN

We employed a mixed methods approach and drew on qualitative research to design a survey instrument to collect consistent flood vulnerability variables that could be pulled into MTurk [46]. Through a literature review of flood risk, we selected variables that are critical in flood risk assessment, particularly those occurring in urban settings [47]–[50]. While the final variables are not exhaustive of all flood-risk factors, we determined that the following list of variables can be collected using GSV imagery and are relevant for Quito. Furthermore, some of these variables, such as building typology, adjacency to other buildings, structure materials, and number of floors (stories), had already been collected from GSV in prior research [7], [51]–[53]. List of variables:

- Number of floors [47], [53]
- Sill height [54]
- Roof type [54]
- Building typology (e.g., residential) [51]
- Street material (e.g., cobble, gravel) [47]

- Structure attached to adjacent building [52]
- Building material [7]
- Overall building condition [47]
- Occupancy status
- Street slope [47]

To ensure consistency in data collection during the turking process, we were faced with the need to standardize variables. The flood vulnerability variables are classified in a codebook consisting of a written definition and reference images. The authors select the GSV reference images for each variable from several global case studies in order to create a codebook that is relevant for all regions. Definitions are compiled from common construction industry descriptions, then discussed and agreed upon among the authors. A portion of this codebook is shown in Table 1 below while the entirety can be found in Supplemental Table I.

We developed a simple HTML script to collect these variables through the mechanical turk process. Turkers are able to view the satellite remote sensing imagery simultaneously with its Google Street View of each sample location. The script can be modified when adjustments to the survey are needed and distributed to all participants to run the modules on their own local computers.

B. SELECTION OF SAMPLE SITES

We generated 500 random sample points inside the district boundaries of Quito in ArcGIS. These points were exported as a delimited text file and distributed between four GIS users to ensure that each point is near a building and has GSV coverage in order to complete the turking process. A high-resolution remote sensing layer was used to observe if the points were near building locations. If a point was not near a building location, it was moved to the closest buildings. We also verified that the points were located close to buildings with GSV coverage. If a GSV coverage and building layer are available, then this process could be expedited by constraining the random point generation to within a buffer of the layers.

C. MTURK SETUP

Turking is a form of crowdsourcing which breaks down tasks into simpler components. These focused tasks are then distributed to multiple individuals. The turking platform facilitates a convenient approach to respond to the tasks and record the inputs [29]. Turking approaches have had a wide range of applications, from assessing comprehensibility of medical pictograms [60] to studying sidewalk accessibility problems in concert with GSV [61]. Turking approaches can also be informed by traditional survey methods to ensure that appropriate questions are being asked.

Our setup for MTurk requires input of the survey template we designed through the literature and the 500 geographic coordinates of our sampled points. In addition, we export an image of a high-resolution satellite remote sensing basemap for each point from ArcGIS using Data Driven Pages to capture each footprint at an appropriate scale to view the building.

TABLE 1. Codebook Definitions of Select Variables Collected Through the Turking Process

<p>Variable 1: Building conditions measuring the functionality of the structure.</p> <p>(1) Very poor: Requires major restoration with possible need to overhaul building subsystems. The approximate restoration cost is 45–60% of building replacement value [55].</p> <p>(2) Poor: Requires significant updating or restoration. The approximate restoration cost is 30–45% of building replacement value. The physical conditions adversely affect building operations [55].</p> <p>(3) Fair: Requires updating or restoration. The approximate restoration cost is 15–30% of building replacement value. The physical conditions may influence building operations [55].</p> <p>(4) Good with minor defects: The approximate restoration cost is 5-15% of building replacement value [55].</p> <p>(5) Very Good: The approximate restoration cost is less than 5% of building replacement value [55].</p>
<p>Variable 2: Type of roofing material, as an indicator of socioeconomic status.</p> <p>(1) Corrugated metal: Galvanized sheet iron or sheet steel shaped into straight parallel regular and equally curved ridges and hollows [56].</p> <p>(2) Tile: Roof tiles are often made from local materials such as terracotta or slate. Modern materials such as concrete, metal and plastic are common, and some clay tiles have a waterproof glaze [57].</p> <p>(3) Thatched, or palm leaves: Roof with dry vegetation such as straw, water reed, sedge, rushes, heather, or palm branches [58].</p> <p>(4) Gravel: layer added to the “build-up roof.” A layer of gravel, or small stones, is applied on top of the final coating of asphalt to protect the roof from the elements, including ultraviolet (UV) rays and hail. The gravel is embedded into the topcoat of asphalt, which helps the gravel to stay in place [59].</p>

These images are loaded into Amazon Web Services (AWS) as data to be accessed by link from MTurk.

We installed a local version of MTurk by Danvk [45] through GitHub that enables the automated turking setup on your own computer. We decided to use this environment to increase the likelihood of consistent results from trained users

The screenshot shows a web-based survey form titled "Building / Structure Information". It contains several sections of questions:

- Select a Sill Height:** Radio buttons for "None, Ground Level", "Low, 1-6\"", "Medium, 7-12\"", "High, 12-18\"", and "Not Applicable".
- Detached / Attached:** Radio buttons for "Detached", "Semi-detached", "Attached", and "Not Applicable".
- Number of Floors:** A numeric input field with a spinner.
- Building Condition, Status and Material:** Radio buttons for "Very Poor", "Poor", "Fair", "Good with Minor Defects", and "Very Good". Below are checkboxes for "Under Construction", "Masonry or Cinder Block", "Wood Construction", "Brick", and "Steel".
- Occupancy:** Radio buttons for "Occupied", "Vacant", and "Cannot determine occupancy".
- Roof Type:** Radio buttons for "Corrugated Metal", "Tile", "Thatched or Palm Leaves", "Tar", "Gravel", and "Other".
- Land Use:** Radio buttons for "Residential", "Commercial", "Agricultural", "Industrial", "Natural", and "Other".
- Street Information:** Radio buttons for "Flat or Low Slope", "Medium Slope", and "Steep Slope".
- Number of Drains Visible:** A numeric input field with a spinner.
- Paved Street (Asphalt):** Radio buttons for "Paved Street (Asphalt)", "Cobble or Cement Blocks", "Dirt or Gravel", "Potholes", and "Other".
- Google StreetView:** Radio buttons for "Google StreetView Available" and "Google StreetView Not Available".

There are also "Additional Notes" text areas and a "Submit" button at the bottom.

FIGURE 2. Turking survey interface.

in our group of GIS specialists. This set up design allowed us to continue the development of the survey questions and ensure that the results would be deemed as reasonable.

We ran the local MTurk module with the template task script for our locations of interest. As shown in Fig. 2, the survey document interface uses the HTML template task script that pulls from the list of sample sites and includes both the AWS link to the footprint image and a link to GSV for the turkers to review the area further.

D. DATA COLLECTION AND ANALYSIS

The team collected data at each geographic coordinate marked sample site point by examining the corresponding GSV image and recording variable characteristics using our survey. Some responses allowed for a free form “Other” response if the selection was not available. In certain cases, the team found that open responses were sufficiently common to justify an updating of the survey template to incorporate these changes.

We evaluated the data collected for each variable through exploratory analysis, mapping, and statistical methods. This step ensured the reasonableness of the variables and provided checks in a few spots in GIS. We visualized the collected data in ArcGIS to identify initial spatial patterns of the flood vulnerability variables (e.g., number of drains in Fig. 4). Finally, we performed inter-rater agreement and intraclass correlation to evaluate consistency for a sample.

While validity is about the accuracy of a measure, reliability indicates the consistency of a measure [62]. The method used in this study is inter-rater reliability, which calculates a

measure of agreement that the same response is obtained by more than one rater [63]. Reliability values range from 0 to 1, and values closer to 1 indicate greater reliability [64]. Two methods were needed to calculate the statistical reliability due to having variables with different data types. Since our data consisted of categorical, ordinal, and continuous data types, two different reliability methods are used; the Fleiss' kappa [65] is applied for the categorical and ordinal data, and the Intraclass Correlation Coefficient (ICC) is applied for the continuous data [66].

First, Fleiss' kappa is a measure of inter-rater agreement used to determine the level of agreement between two or more raters in which the data are categorical or ordinal [67]. Fleiss' kappa is a modified version of Cohen's kappa used for more than two raters [68]. We used the inter-rater agreement Fleiss method since there were four evaluators.

Second, for continuous variables, the ICC is used instead. This study considered three factors: 1) model, 2) type selection, and 3) definition selection to determine which ICC model best suits the study's needs. The ICC model determined as the most appropriate was the two-way random effects, absolute agreement, and multiple raters/measurement, known as the ICC (2, k) [47]. The ICC (2, k) formula ($MS_{\text{rows}} - MS_{\text{error}}/MS_{\text{rows}}$) is used to calculate intraclass correlation based on two-way random effects for consistency between multiple raters/measurement. The interrater was calculated for nine variables, while the intraclass correlation was calculated for two variables (e.g., number of drains and floors).

The research team collected data on the same 50 locations from the 500 randomly sampled images of Quito, Ecuador. Each researcher independently rated each image based on sill height, building structure, number of floors, building/house material, occupancy, roof type, land use, slope, number of drains, and street description, etc. Thus, one researchers' judgment did not affect another researcher's judgment and choice. However, a codebook was developed beforehand to specify how to categorize each variable and promote consistency. Each rater had the same number of categories to choose from with mutually exclusive categories. For example, sill height categories were none, low, medium, and high. Raters could select building structures as either semi-detached, detached, or inapplicable, and building conditions were categorized by poor, fair, good, or very good. Roof types, classified as being either gravel, tile, corrugated metal, or hatched leaves. Land use categorical description options were commercial, residential, natural, or industrial. The slope was defined as either none/low, medium, or high, and the street description was categorized as paved and with potholes. Fleiss' kappa was applied to the aforementioned categorical variables. The ICC (2, k) was applied to the number of drains and the number of floors as they are the only continuous data in this study.

III. RESULTS

The mechanical turking approach resulted in an alternative to the utilization of on-the-ground field surveys. We collected

32 / 101



FIGURE 3. Example of building point with corresponding remote sensing image and GSV.

data for 458 points in Quito and were unable to collect data for 42 points, either because the sampled points were duplicated by being too close together or GSV coverage was not available. In the present case study for Quito, the average time for the turking process was 3–5 minutes per point with each location having 12 variables to collect.

The top half of Fig. 3 shows an overview of the surroundings from a satellite imagery basemap. This image helps to add context about the building location and environment. The bottom half of Fig. 3 shows a GSV panoramic image, for the same location, that can be used to move along the street similar to a Google Map environment. Viewing both the satellite and street-level views helped the collection of data about the roof type, street material, land use, and slope. Navigating the street with the coverage provided by GSV particularly allowed for the collection of information about the sill height, slope, number of drains, building condition and material, and number of floors.

The data collected about the variables were visualized as seen in Figs. 4 and 5. These are just two examples to demonstrate the data that were collected. The visualizations illustrate the ability to quickly capture characteristics of the city relevant to flooding from anywhere GSV is available.

The map depicted in Fig. 4 shows the number of drains found at each point surveyed through the mechanical turking process. The darkest blue points show locations of buildings where drains were not visible at the street level, suggesting a lack of drains along the periphery of the city. In particular, the southwest part of Quito shows an area of low density of drains in areas that are populated. This could indicate a higher grade of vulnerability to flooding in that area. The light blue colored points represent the location of buildings where drains were

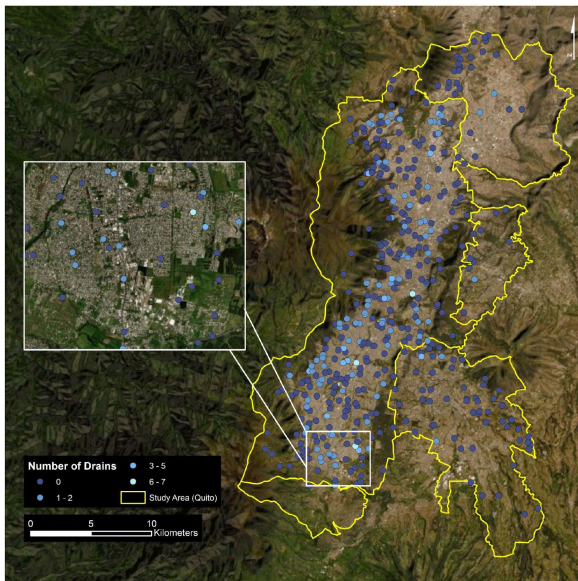


FIGURE 4. Map of variable collected on number of drains visible at specific point locations.

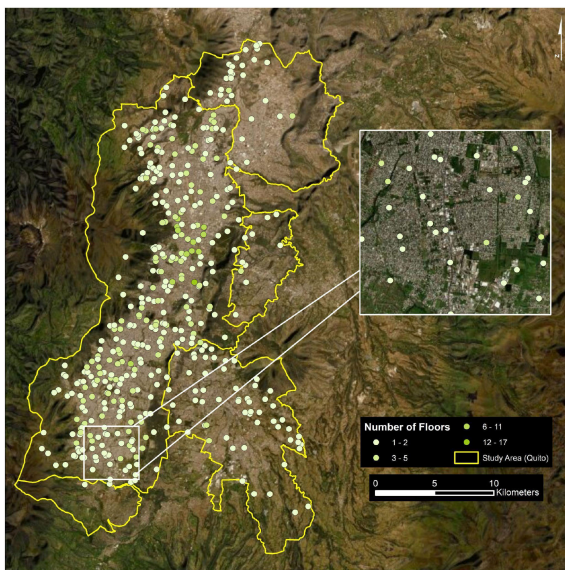


FIGURE 5. Map of observations collected on the number of floors at point locations.

visible; most of these occur close to the center of the city of Quito.

Fig. 5 shows the spatial distribution of the sampled buildings, with darker green representing buildings with more floors (stories) and lighter green indicating those with fewer floors. The periphery of the city, in particular the southeastern part of Quito in the inset, shows a cluster of low-height buildings but almost no taller buildings. The spatial distribution of this data across Quito is valuable for flood risk assessment as the number of floors is a commonly used variable [47].

TABLE 2. Summary of Variables By Data Type (Categorical = Yellow, Ordinal = Blue, Continuous = Red) with List of Categories for Each Variable and Number of Categories

Variable	Entry Options	#
Building Material	Masonry/Cinder Block, Wood, Brick, and Steel	4
Roof Type	Corrugated Metal, Tile, Thatched or Palm Leaves, Tar, Gravel, Concrete, and two or more categories	7
Street Type	Asphalt, Cobble or Cement, Dirt or Gravel, Pothole	4
Land Use	Residential, Commercial, Natural, Agricultural, and two or more categories	5
Structure Type	Detached, Semi-Detached, Attached, Non-Applicable	4
Occupancy Status	Occupied, Vacant, and Cannot Determine Occupancy	3
Sill Height	Ground Level, Low (1-6), Medium (7-12), High (12-18)	4
Building Condition	Very Poor, Poor, Fair, Good with Minor Defects, and Very Good	5
Street Topography	Flat or Low Slope, Medium Slope, Steep Slope	3
Floors	Number of Floors	7
Drains	Number of Drains	17

The data we collected are relevant for analysis of flood risk in Quito. For example, the number of drains (Fig. 4) relates to the status of existing infrastructure to counter floods surrounding a building. cursory observation of Fig. 4 demonstrates that drain coverage varies greatly in Quito - some areas lack drains while others have several. This variability in infrastructure is relevant for decision-makers and emergency management, allowing them to take into account building and street-level variables for spatial flood risk assessment. Furthermore, the ease of data collection without the need for in-situ observation potentially reduces the financial and capacity burden for emergency management.

Finally, a codebook was produced to describe the meaning of the variable categories to facilitate consistency in rating. Each observer used this codebook as a reference guide. A selection of the variables is shown in Table 2 with their data type and category options.

Next, the results were accumulated, and the average is given for the overall score. The overall kappa agreement for this study was moderate to substantial between the four observers with a $\kappa = .79$. The kappa agreement for each category ranges from .54 to .98 (see Table 3). The kappa statistic is influenced by disagreement among classes with a low prevalence of responses, see Supplementary Table II for the breakdown of responses per variable.

We found that low kappa levels were often due to individual raters selecting two or more categories for a particular variable. For example, one rater can choose that the roof type has corrugated metal and cement, while another can only select

TABLE 3. Calculation of Interrater Reliability Kappa Result

Variable	Kappa (κ)
Building Material	0.94
Roof Type	0.83
Street Type	0.87
Land Use	0.88
Structure Type	0.64
Occupancy Status	0.80
Sill Height	0.66
Building Condition	0.54
Street Topography	0.79
<i>Sum without intraclass correlation</i>	
	6.94
Number of variables	9
<i>Interrater without intraclass correlation</i>	0.77
Floors	0.98
Drains	0.80
<i>Sum with intraclass correlation</i>	
	8.73
Number of variables	11
<i>Interrater with intraclass correlation</i>	0.79

cement. One could improve this score by only permitting the selection of one category and providing a more conservative selection. This could mean only distinguishing between categories that produce higher flood vulnerability for that variable. Another issue that arose with our survey was the distinction between categories that are more similar than different such as very good or good when specifying building condition. This level of specification may not be appropriate for a rater to determine. An appropriate solution for future work is to collapse the building conditions into three more distinct and well described categories. This approach would improve the agreement scores between evaluators and improve the quality of the training data as there would not be as many artificial distinctions.

IV. DISCUSSION

We see certain advantages of incorporating social factors from the street-level data collection and modeling for humanitarian mapping as opposed to traditional hydrologic/hydraulic engineering approaches. Typical hydrologic models for urban

flooding provide a spatial map of runoff depth and discharge that helps to plan engineering intervention to reduce flood risk. The advantage of collecting crowdsourced street-level data is that it directly reflects the observable conditions of the area (e.g., roof type, building material, building condition, sill height, presence of drains, street inclination). The features relevant to flood vulnerability vary by geographic area and conditions. Therefore, for this method to be applied to other areas, it can be appropriate to update the variables extracted upon further inspection of the region and feedback from those with local knowledge.

We found that the presence of drains in Quito, which could provide flood protection, were associated with proximity to the center of the study area. As the results demonstrated, many of the sample points where no drains were spotted are along the periphery of the city. This is consistent with the nature of urban sprawl in Latin American cities [69], [70] and informal settlements in fast growing urban areas such as Quito. Similarly, the spatial distribution of buildings with a higher number of floors were found to be associated with proximity to the city center. We also found clusters of buildings with less than five stories in the southern, particularly southeastern regions of Quito. The development of the southern fringe is characterized by one- or two-story buildings which makes the area highly vulnerable to flooding. The agreement in the findings of the team members on these variables demonstrate a degree of reliability in the data collected. Further work is needed to tease out the intersection of vulnerability related factors. For example, high poverty areas might not have high sills at the doorsteps and are likely to be located on steep slopes at the periphery of Quito with poor construction.

This paper shows that vulnerability variables collected from GSV by multiple team members for the sample points showed consistency. This is an important component in our research because this method is intended to serve as a way to develop training data for modeling which should be evaluated prior to generalizing. Our case study presents a method for the evaluation of the remote visual inspections made by the raters through an inter-rater agreement and intraclass step. The result of the evaluation shows a moderate to substantial statistical agreement between the team for the variables of interest and could help to direct users to more consistent variable measures to obtain higher levels of accuracy. Finally, one should evaluate the generalizability of the data through mapping of the spatial data to identify errors or patterns of interest.

Integration of hydrologic models and social vulnerability characteristics could provide an ideal framework for flood vulnerability mapping. The hydrologic/hydraulic process requires significant resources to collect all the necessary data along with consequent model calibration and verification. From this point of view, the process for collecting data from GSV is perhaps faster to implement for humanitarian purposes and feasible to accomplish remotely. The data could then be

used alongside flood observations and models, or other hazard layers.

Unfortunately, comprehensive GSV coverage of streets does not exist globally as many areas lack collection, particularly in the developing world and in rural areas. A concern is that these areas are those in which flood risk assessment and flood anticipatory action programs are most needed [71]. However, in our case study of Quito, we found that there was sufficient coverage.

While GSV coverage is extensive across Quito, it is not available for every building. The team often encountered buildings without corresponding GSV imagery which resulted in the final collection of variables for 458 points out of 500. Also, some variables were more difficult to collect than others. For instance, roof material type was not always visible from GSV. Assessing street slope from GSV also proved challenging, particularly when distinguishing between low and medium slopes. Finally, some aspects of buildings such as the interior of the structures cannot be captured from a street view.

We also encountered limitations in the view from the street due to physical barriers. In Quito, many residential and commercial buildings have high walls around them resulting in an inability to view the complete building via GSV. This prevented an accurate assessment of the physical structure of the buildings. During our background research we noticed the mention of geotagging inaccuracies when attempting to locate structures in GSV based on addresses [7]. Our study however used coordinates rather than street addresses to locate buildings. These issues should be considered when determining how to use GSV to derive data.

It is noted that the methods presented here will have limitations on where they will be applicable, and further, we note that data quality using GSV may vary even in areas where it is available; therefore, careful consideration must be taken to ensure that appropriate adjustments for standardized collection are made. These adjustments could include moving the previously generated points to areas with available GSV. The lack of images in certain places may be a result of a sampling bias in GSV collection despite the randomized method used in this study and could cause an unintended misrepresentation of study areas. Therefore, we carefully evaluated the data we collected to ensure there was sufficient spatial coverage in the end. In terms of the consistency of variable collection, we found that a level of subjective interpretation during turking is unavoidable even after standardization of variable descriptions.

Despite the current limitations on GSV coverage globally, we believe that there is the potential to continue to expand this approach to other urban areas. With the addition of new resources and ways of collecting, Google is expanding its coverage every year [72]. Google Street View trekkers is a program that provides camera equipment to volunteer professional photographers and other individuals to collect GSV images [73]. In addition, one can hire trusted professionals to produce Street View in particular areas [74]. There is also

a Street View app in which anyone can collect GSV through mobile devices and upload a path [72]. These alternative ways of inputting data can reduce some of the barriers of coverage, provide the ability to task coverage in areas of interest, and open more areas for assessment.

V. CONCLUSION

Natural hazard driven disasters [75] disproportionately impact vulnerable populations who are often not represented on a map [76]. A lack of data, or a lack of data of a sufficient quality, leads to challenges in various decision-making contexts, including it being particularly challenging to design risk-based anticipatory action programs, especially in complex settings such as those involving migration, displacement and informal settlements [77]. We present a crowdsourcing method using a human-machine interface to map characteristics of the built infrastructure that also provide socioeconomic context relevant to flood vulnerability in urban areas. This work shows that we can use remote collection techniques to capture information on vulnerability which is otherwise unavailable, infrequent, or would require time-consuming and expensive field studies. We learned that we can quickly capture flood vulnerability variables on hundreds of buildings in a few hours based on visual inspection; however, it is important to evaluate the uncertainty in the outputs of the process.

While this paper focuses on Quito, Ecuador as a case study, the methodology can be quickly replicated to produce and evaluate labeled training data in other areas. We developed a method to ensure that the data collected and the trends within cities are consistent. The long-term goal of this project is to build training datasets for urban areas for global regions that will allow us to automate the mapping of flood vulnerability in the future. We found that the mapping of the variables collected along with other datasets on the same topics, such as the slope variable mapped with an elevation layer is informative to evaluate reliability. Our approach needs to show consistency amongst the team which is why the standardized codebook was developed to encourage a common understanding and statistical reliability measures were used to evaluate the quality of variables. We believe that the project could be expanded to the online MTurk platform once the project is fully developed and if user training is provided on using the codebook for standardization.

Further work comparing data collected through our MTurk approach with census microdata at the building level through field studies would complement this initial exercise. However, the availability of detailed microdata is limited and is not available for Quito, Ecuador. We are developing a separate case study in Colombia that compares official field study microdata from the national census to further validate the collection of the labeled data. In addition, our method could be adapted for participatory GIS approaches with community partners to target specific areas of interest for evaluation of the outputs based on local knowledge.

This method for collection along with the upcoming evaluation steps and the expansion of this project lead the way for remote collection of street-level variables to contribute valuable information on vulnerability for humanitarian action. High resolution information on factors affecting flood vulnerability can be an invaluable resource for all stages of the disaster management cycle. The ability to collect data quickly and remotely on street-level conditions could be a game changer for decision makers. We believe that the use of novel geospatial technologies is an emerging research area that will have significant implications for humanitarian policy as high-resolution data become timelier and more accessible.

REFERENCES

- [1] S. Y. Cho and H. Chang, "Recent research approaches to urban flood vulnerability, 2006–2016," *Nat. Hazards*, vol. 88, no. 1, pp. 633–649, Aug. 2017, doi: [10.1007/s11069-017-2869-4](https://doi.org/10.1007/s11069-017-2869-4).
- [2] United Nations, Department of Economic and Social Affairs, "World urbanization prospects: The 2018 revision (key facts)," 2018, Accessed: Feb. 2022. [Online]. Available: <https://www.un.org/development/desa/publications/2018-revision-of-world-urbanization-prospects.html>
- [3] S. Shrestha, S. Cui, L. Xu, L. Wang, B. Manandhar, and S. Ding, "Impact of land use change due to urbanisation on surface runoff using GIS-based SCS-CN method: A case study of Xiamen city, China," *Land*, vol. 10, no. 8, Aug. 2021, Art. no. 839, doi: [10.3390/land10080839](https://doi.org/10.3390/land10080839).
- [4] B. R. Rosenzweig *et al.*, "Pluvial flood risk and opportunities for resilience," *WIREs Water*, vol. 5, no. 6, Nov. 2018, Art. no. e1302, doi: [10.1002/wat2.1302](https://doi.org/10.1002/wat2.1302).
- [5] S. Pande and M. Sivapalan, "Progress in socio-hydrology: A meta-analysis of challenges and opportunities," *WIREs Water*, vol. 4, no. 4, Jul. 2017, Art. no. e1193, doi: [10.1002/wat2.1193](https://doi.org/10.1002/wat2.1193).
- [6] S. Etinger *et al.*, "Building vulnerability to hydro-geomorphic hazards: Estimating damage probability from qualitative vulnerability assessment using logistic regression," *J. Hydrol.*, vol. 541, pp. 563–581, Oct. 2016, doi: [10.1016/j.jhydrol.2015.04.017](https://doi.org/10.1016/j.jhydrol.2015.04.017).
- [7] M. Diakakis, G. Deligiannakis, A. Pallikarakis, and M. Skordoulis, "Identifying elements that affect the probability of buildings to suffer flooding in urban areas using google street view. A case study from athens metropolitan area in Greece," *Int. J. Disaster Risk Reduct.*, vol. 22, pp. 1–9, Jun. 2017, doi: [10.1016/j.ijdr.2017.02.002](https://doi.org/10.1016/j.ijdr.2017.02.002).
- [8] C. Wang *et al.*, "Analyzing explanatory factors of urban pluvial floods in Shanghai using geographically weighted regression," *Stoch. Environ. Res. Risk Assess.*, vol. 31, no. 7, pp. 1777–1790, Sep. 2017, doi: [10.1007/s00477-016-1242-6](https://doi.org/10.1007/s00477-016-1242-6).
- [9] G. Romanescu, O. E. Hapciuc, I. Minea, and M. Iosub, "Flood vulnerability assessment in the mountain–plateau transition zone: A case study of Marginea village (Romania)," *J. Flood Risk Manage.*, vol. 11, pp. S502–S513, 2018, doi: [10.1111/jfr3.12249](https://doi.org/10.1111/jfr3.12249).
- [10] B. R. Rosenzweig *et al.*, "The value of urban flood modeling," *Earth's Future*, vol. 9, no. 1, Jan. 2021, doi: [10.1029/2020EF001739](https://doi.org/10.1029/2020EF001739).
- [11] H. Chang *et al.*, "Assessment of urban flood vulnerability using the social-ecological-technological systems framework in six US cities," *Sustain. Cities Soc.*, vol. 68, May 2021, Art. no. 102786, doi: [10.1016/j.scs.2021.102786](https://doi.org/10.1016/j.scs.2021.102786).
- [12] K. Karagiorgos, T. Thaler, M. Heiser, J. Hübl, and S. Fuchs, "Integrated flash flood vulnerability assessment: Insights from east attica, Greece," *J. Hydrol.*, vol. 541, pp. 553–562, Oct. 2016, doi: [10.1016/j.jhydrol.2016.02.052](https://doi.org/10.1016/j.jhydrol.2016.02.052).
- [13] W. Yang, K. Xu, J. Lian, L. Bin, and C. Ma, "Multiple flood vulnerability assessment approach based on fuzzy comprehensive evaluation method and coordinated development degree model," *J. Environ. Manage.*, vol. 213, pp. 440–450, May 2018, doi: [10.1016/j.jenvman.2018.02.085](https://doi.org/10.1016/j.jenvman.2018.02.085).
- [14] M. Paphathoma-Köhle, "Vulnerability curves vs. vulnerability indicators: Application of an indicator-based methodology for debris-flow hazards," *Nat. Hazards Earth Syst. Sci.*, vol. 16, no. 8, pp. 1771–1790, Aug. 2016, doi: [10.5194/nhess-16-1771-2016](https://doi.org/10.5194/nhess-16-1771-2016).
- [15] C. Arrighi, B. Mazzanti, F. Pistone, and F. Castelli, "Empirical flash flood vulnerability functions for residential buildings," *SN Appl. Sci.*, vol. 2, no. 5, May 2020, Art. no. 904, doi: [10.1007/s42452-020-2696-1](https://doi.org/10.1007/s42452-020-2696-1).
- [16] F. Carisi, K. Schröter, A. Domeneghetti, H. Kreibich, and A. Castellarin, "Development and assessment of uni- and multivariable flood loss models for Emilia-Romagna (Italy)," *Nat. Hazards Earth Syst. Sci.*, vol. 18, no. 7, pp. 2057–2079, Jul. 2018, doi: [10.5194/nhess-18-2057-2018](https://doi.org/10.5194/nhess-18-2057-2018).
- [17] A. Karmaoui, S. Zerouali, H. A. Ougougdal, and A. A. Shah, "A new mountain flood vulnerability index (MFVI) for the assessment of flood vulnerability," *Sustain. Water Resour. Manag.*, vol. 7, no. 6, Dec. 2021, Art. no. 92, doi: [10.1007/s40899-021-00575-z](https://doi.org/10.1007/s40899-021-00575-z).
- [18] H. Nasiri, M. J. M. Yusof, T. A. M. Ali, and M. K. B. Hussein, "District flood vulnerability index: Urban decision-making tool," *Int. J. Environ. Sci. Technol.*, vol. 16, no. 5, pp. 2249–2258, May 2019, doi: [10.1007/s13762-018-1797-5](https://doi.org/10.1007/s13762-018-1797-5).
- [19] M. Zhang, W. Xiang, M. Chen, and Z. Mao, "Measuring social vulnerability to flood disasters in China," *Sustainability*, vol. 10, no. 8, Jul. 2018, Art. no. 2676, doi: [10.3390/su10082676](https://doi.org/10.3390/su10082676).
- [20] M. Dilley *et al.*, "Natural disaster hotspots: A global risk analysis," *World Bank*, Washington, D.C, USA, 2005. [Online]. Available: <https://openknowledge.worldbank.org/handle/10986/7376>
- [21] World Bank, "Disaster risk management in latin america and the caribbean region: GFDRR country notes." World Bank, 2012, doi: [10.1596/27336](https://doi.org/10.1596/27336).
- [22] World Population Review, "Quito population 2021." [Online]. Available: <https://worldpopulationreview.com/world-cities/quito-population>, (accessed Sep. 17, 2021).
- [23] I. Loor and J. Evans, "Understanding the value and vulnerability of informal infrastructures: Footpaths in quito," *J. Transp. Geogr.*, vol. 94, Jun. 2021, Art. no. 103112, doi: [10.1016/j.jtrangeo.2021.103112](https://doi.org/10.1016/j.jtrangeo.2021.103112).
- [24] A. G. Salazar and N. Cui, "Asentamientos informales y medio ambiente en quito," *Áreas Rev. Int. Cienc. Soc.*, vol. 35, no. 2016, pp. 101–119, 2016. [Online]. Available: <https://revistas.um.es/areas/article/view/279181/204161>
- [25] J. Pinos and L. Timbe, "Mountain riverine floods in Ecuador: Issues, challenges, and opportunities," *Front. Water*, vol. 2, Oct. 2020, Art. no. 545880, doi: [10.3389/frwa.2020.545880](https://doi.org/10.3389/frwa.2020.545880).
- [26] J. Lhomme, C. Bouvier, and J. Perrin, "Applying a GIS-based geomorphological routing model in urban catchments," *J. Hydrol.*, vol. 299, no. 3–4, pp. 203–216, Dec. 2004, doi: [10.1016/S0022-1694\(04\)00367-1](https://doi.org/10.1016/S0022-1694(04)00367-1).
- [27] Google, "Google street view." *Street View*. [Online]. Available: <https://www.google.com/streetview/>
- [28] Esri *et al.*, "World imagery map," 2009, [Online]. Available: <https://www.arcgis.com/home/item.html?id=10df2279f9684e4a9f6a7f08feba2a9>
- [29] Amazon, "Amazon mechanical turk." [Online]. Available: <https://www.mturk.com>
- [30] GuaiFai, "Quito, guayaquil, cuenca y más ya son parte de google street view," *El Comercio*, Nov. 16, 2015. [Online]. Available: <https://www.elcomercio.com/guafai/quito-guayaquil-google-maps-streetview.html>
- [31] Jamie, "How often does google street view update," Mar. 1, 2021. [Online]. Available: <https://www.alphr.com/how-often-google-street-view-update/>
- [32] C. Gartenberg, "Google reveals just how much of the world it's mapped with street view and earth," *The Verge*, Dec. 13, 2019. [Online]. Available: <https://www.theverge.com/2019/12/13/21020814/google-world-mapped-street-view-earth-square-miles>
- [33] R. Nieva, "Google maps has now photographed 10 million miles in street view," *CNET*, Dec. 13, 2019. [Online]. Available: <https://www.cnet.com/news/google-maps-has-now-photographed-10-million-miles-in-street-view/>
- [34] D. Fry, S. J. Mooney, D. A. Rodríguez, W. T. Caiaffa, and G. S. Lovasi, "Assessing google street view image availability in latin american cities," *J. Urban Health*, vol. 97, no. 4, pp. 552–560, Aug. 2020, doi: [10.1007/s11524-019-00408-7](https://doi.org/10.1007/s11524-019-00408-7).
- [35] H. M. Badland, S. Opit, K. Witten, R. A. Kearns, and S. Mavoia, "Can virtual streetscape audits reliably replace physical streetscape audits?," *J. Urban Health*, vol. 87, no. 6, pp. 1007–1016, Dec. 2010, doi: [10.1007/s11524-010-9505-x](https://doi.org/10.1007/s11524-010-9505-x).

- [36] A. G. Rundle, M. D. M. Bader, C. A. Richards, K. M. Neckerman, and J. O. Teitler, "Using google street view to audit neighborhood environments," *Amer. J. Prev. Med.*, vol. 40, no. 1, pp. 94–100, Jan. 2011, doi: [10.1016/j.amepre.2010.09.034](https://doi.org/10.1016/j.amepre.2010.09.034).
- [37] B. T. Taylor, P. Fernando, A. E. Bauman, A. Williamson, J. C. Craig, and S. Redman, "Measuring the quality of public open space using Google Earth," *Amer. J. Prev. Med.*, vol. 40, no. 2, pp. 105–112, Feb. 2011, doi: [10.1016/j.amepre.2010.10.024](https://doi.org/10.1016/j.amepre.2010.10.024).
- [38] J. S. Wilson *et al.*, "Assessing the built environment using omnidirectional imagery," *Amer. J. Prev. Med.*, vol. 42, no. 2, pp. 193–199, Feb. 2012, doi: [10.1016/j.amepre.2011.09.029](https://doi.org/10.1016/j.amepre.2011.09.029).
- [39] M. D. M. Bader *et al.*, "Development and deployment of the computer assisted neighborhood visual assessment system (CANVAS) to measure health-related neighborhood conditions," *Health Place*, vol. 31, pp. 163–172, Jan. 2015, doi: [10.1016/j.healthplace.2014.10.012](https://doi.org/10.1016/j.healthplace.2014.10.012).
- [40] J. J. Plascak *et al.*, "Drop-and-spin virtual neighborhood auditing: Assessing built environment for linkage to health studies," *Amer. J. Prev. Med.*, vol. 58, no. 1, pp. 152–160, Jan. 2020, doi: [10.1016/j.amepre.2019.08.032](https://doi.org/10.1016/j.amepre.2019.08.032).
- [41] C. M. Smith, J. D. Kaufman, and S. J. Mooney, "Google street view image availability in the Bronx and San Diego, 2007–2020: Understanding potential biases in virtual audits of urban built environments," *Health Place*, vol. 72, Nov. 2021, Art. no. 102701, doi: [10.1016/j.healthplace.2021.102701](https://doi.org/10.1016/j.healthplace.2021.102701).
- [42] M. Aahlaad, C. Mozumder, N. Tripathi, and I. Pal, "An object-based image analysis of worldview-3 image for urban flood vulnerability assessment and dissemination through ESRI story maps," *J. Indian Soc. Remote Sens.*, vol. 49, no. 11, pp. 2639–2654, Nov. 2021, doi: [10.1007/s12524-021-01416-4](https://doi.org/10.1007/s12524-021-01416-4).
- [43] R. B. Mostafiz *et al.*, "Comparison of neighborhood-scale, residential property flood-loss assessment methodologies," *Front. Environ. Sci.*, vol. 9, Oct. 2021, Art. no. 734294, doi: [10.3389/fenvs.2021.734294](https://doi.org/10.3389/fenvs.2021.734294).
- [44] H. Ning, Z. Li, X. Ye, S. Wang, W. Wang, and X. Huang, "Exploring the vertical dimension of street view image based on deep learning: A case study on lowest floor elevation estimation," *Int. J. Geogr. Inf. Sci.*, pp. 1–26, Oct. 2021, doi: [10.1080/13658816.2021.1981334](https://doi.org/10.1080/13658816.2021.1981334).
- [45] Danvk, *Local Turk*, 2018. [Online]. Available: <https://github.com/danvk/localturk>
- [46] J. Schoonenboom and R. B. Johnson, "How to construct a mixed methods research design," *KZfSS Köln. Z. Für Sozial. Sozialpsychologie*, vol. 69, no. S2, pp. 107–131, Oct. 2017, doi: [10.1007/s11577-017-0454-1](https://doi.org/10.1007/s11577-017-0454-1).
- [47] M. Fedeski and J. Gwilliam, "Urban sustainability in the presence of flood and geological hazards: The development of a GIS-based vulnerability and risk assessment methodology," *Landsc. Urban Plan.*, vol. 83, no. 1, pp. 50–61, Nov. 2007, doi: [10.1016/j.landurbplan.2007.05.012](https://doi.org/10.1016/j.landurbplan.2007.05.012).
- [48] M. Pregnolato, A. Ford, C. Robson, V. Glenis, S. Barr, and R. Dawson, "Assessing urban strategies for reducing the impacts of extreme weather on infrastructure networks," *R. Soc. Open Sci.*, vol. 3, no. 5, May 2016, Art. no. 160023, doi: [10.1098/rsos.160023](https://doi.org/10.1098/rsos.160023).
- [49] H. Skilodimou, G. Livaditis, G. Bathrellos, and E. Verikiou-papaspiridakou, "Investigating the flooding events of the urban regions of glyfada and voula, attica, Greece: A contribution to urban geomorphology," *Geogr. Ann. Ser. Phys. Geogr.*, vol. 85, no. 2, pp. 197–204, Jun. 2003, doi: [10.1111/1468-0459.00198](https://doi.org/10.1111/1468-0459.00198).
- [50] L. Zambrano, R. Pacheco-Muñoz, and T. Fernández, "Influence of solid waste and topography on urban floods: The case of Mexico city," *Ambio*, vol. 47, no. 7, pp. 771–780, Nov. 2018, doi: [10.1007/s13280-018-1023-1](https://doi.org/10.1007/s13280-018-1023-1).
- [51] A. E. Jiménez and R. A. Cubillos, "Perceived stress and job satisfaction after the earthquake of february 27 2010 occurred in the central-south zone of Chile," *Ter. Psicol.*, vol. 28, no. 2, pp. 187–192, 2010, [Online]. Available: <http://teps.cl/index.php/teps/article/view/198>
- [52] A. Blanco-Vogt and J. Schanze, "Assessment of the physical flood susceptibility of buildings on a large scale – conceptual and methodological frameworks," *Nat. Hazards Earth Syst. Sci.*, vol. 14, no. 8, pp. 2105–2117, Aug. 2014, doi: [10.5194/nhess-14-2105-2014](https://doi.org/10.5194/nhess-14-2105-2014).
- [53] A. Mollaei, N. Ibrahim, and K. Habib, "Estimating the construction material stocks in two Canadian cities: A case study of kitchener and waterloo," *J. Clean. Prod.*, vol. 280, Jan. 2021, Art. no. 124501, doi: [10.1016/j.jclepro.2020.124501](https://doi.org/10.1016/j.jclepro.2020.124501).
- [54] A. Müller, J. Reiter, and U. Weiland, "Assessment of urban vulnerability towards floods using an indicator-based approach — A case study for Santiago de Chile," *Nat. Hazards Earth Syst. Sci.*, vol. 11, no. 8, pp. 2107–2123, Aug. 2011, doi: [10.5194/nhess-11-2107-2011](https://doi.org/10.5194/nhess-11-2107-2011).
- [55] K. L. Cyros and R. Korb, "Postsecondary education facilities inventory and classification manual (FICM): 2006 edition." National Center for Education Statistics, Institute of Education Sciences, May 2006. [Online]. Available: <https://nces.ed.gov/pubsub/2006/2006160.pdf>
- [56] Merriam Webster Dictionary, "Corrugated iron," *Merriam Webster Dictionary*, [Online]. Available: <https://www.merriam-webster.com/dictionary/corrugated%20iron>
- [57] Wikipedia, "Roof tiles," *Wikipedia*, Accessed: Sep. 17, 2021. [Online]. Available: https://en.wikipedia.org/wiki/Roof_tiles
- [58] Wikipedia, "Thatching," *Wikipedia: the Free Encyclopedia*, Accessed: Sep. 17, 2021. [Online]. Available: <https://en.wikipedia.org/wiki/Thatching#:~:text=Thatching%20is%20the%20craft%20of,away%20from%20the%20inner%20roof>
- [59] Restoration Builders, "A tar & gravel roof guide for beginners (Updated for 2021)," *Restoration Builders*, [Online]. Available: <https://restorbuilders.com/tar-gravel-roof/>
- [60] B. Yu, M. Willis, P. Sun, and J. Wang, "Crowdsourcing participatory evaluation of medical pictograms using amazon mechanical turk," *J. Med. Internet Res.*, vol. 15, no. 6, Jun. 2013, Art. no. 108, doi: [10.2196/jmir.2513](https://doi.org/10.2196/jmir.2513).
- [61] K. Hara, V. Le, and J. Froehlich, "Combining crowdsourcing and google street view to identify street-level accessibility problems," in *Proc. SIGCHI Conf. Hum. Factors Comput. Syst.*, Paris, France, Apr. 2013, pp. 631–640, doi: [10.1145/2470654.2470744](https://doi.org/10.1145/2470654.2470744).
- [62] P. Roberts, H. Priest, and M. Traynor, "Reliability and validity in research," *Nurs. Stand.*, vol. 20, no. 44, pp. 41–45, Jul. 2006, doi: [10.7748/ns.20.44.41.s56](https://doi.org/10.7748/ns.20.44.41.s56).
- [63] M. Syed and S. C. Nelson, "Guidelines for establishing reliability when coding narrative data," *Emerg. Adulthood*, vol. 3, no. 6, pp. 375–387, Dec. 2015, doi: [10.1177/2167696815587648](https://doi.org/10.1177/2167696815587648).
- [64] J. Sim and C. C. Wright, "The kappa statistic in reliability studies: Use, interpretation, and sample size requirements," *Phys. Ther.*, vol. 85, no. 3, pp. 257–268, Mar. 2005, doi: [10.1093/ptj/85.3.257](https://doi.org/10.1093/ptj/85.3.257).
- [65] Zach, "How to calculate fleiss's kappa in excel," *Statology*, Jul. 27, 2020. [Online]. Available: <https://www.statology.org/fleiss-kappa-excel>
- [66] Zach, "Intraclass correlation coefficient: Definition + example," *Statology*, Mar. 19, 2021. [Online]. Available: <https://www.statology.org/intraclass-correlation-coefficient/>
- [67] J. L. Fleiss, "Measuring nominal scale agreement among many raters.," *Psychol. Bull.*, vol. 76, no. 5, pp. 378–382, 1971, doi: [10.1037/h0031619](https://doi.org/10.1037/h0031619).
- [68] M. L. McHugh, "Interrater reliability: The kappa statistic," *Biochem. Medica*, vol. 22, no. 3, pp. 276–282, 2012, doi: [10.11613/BM.2012.031](https://doi.org/10.11613/BM.2012.031).
- [69] E. Salazar, C. Henriquez, G. Durán, J. Quense, and F. Puente-Sotomayor, "How to define a new metropolitan area? The case of quito, Ecuador, and contributions for urban planning," *Land*, vol. 10, no. 4, Apr. 2021, Art. no. 413, doi: [10.3390/land10040413](https://doi.org/10.3390/land10040413).
- [70] B. Reed, "Sustainable urban drainage in low-income countries: A scoping study," Water, Engineering and Development Centre, Loughborough University, Leicestershire, U.K., 2004. Accessed: Feb. 5, 2022. [Online]. Available: https://www.researchgate.net/publication/312951227_Sustainable_Urban_Drainage_in_Low-Income_Countries_-_A_Scoping_Study_Project_Report
- [71] A. Kruczkiewicz *et al.*, "Earth observations for anticipatory action: Case studies in hydrometeorological hazards," Elsevier Ltd., 2021. [Online]. Available: <https://doi.org/10.1016/B978-0-12-819412-6.00011-0>
- [72] T. Warren, "Google maps now lets you create street view photos with just a phone," *The Verge*, Dec. 3, 2021. [Online]. Available: <https://www.theverge.com/2020/12/3/22149884/google-maps-street-view-photos-phone-android-update>
- [73] J. Heimbuch, "How to become a google street view trekker," *Treehugger*, Mar. 16, 2016. [Online]. Available: <http://how-to-do.website/2016/03/31/how-to-become-a-google-street-view-trekker/>
- [74] Google, "Hire a trusted pro, boost your visibility," Street View, [Online]. Available: <https://www.google.co.in/streetview/business/trusted/>
- [75] "No Natural Disasters," *No Natural Disasters*. [Online]. Available: <https://www.nonaturaldisasters.com>, (accessed, Feb. 5, 2022).
- [76] C. Nauman *et al.*, "Perspectives on flood forecast-based early action and opportunities for earth observations," *J. Appl. Remote Sens.*, vol. 15, no. 3, Feb. 2021, Art. no. 032002, doi: [10.1117/1.JRS.15.032002](https://doi.org/10.1117/1.JRS.15.032002).
- [77] A. Kruczkiewicz *et al.*, "Opinion: Compound risks and complex emergencies require new approaches to preparedness," *Proc. Nat. Acad. Sci.*, vol. 118, no. 19, May 2021, Art. no. 2106795118, doi: [10.1073/pnas.2106795118](https://doi.org/10.1073/pnas.2106795118).

RAYCHELL VELEZ received the B.A. degree in biology and the M.S. degree in geographic information science from the City University of New York, Lehman College, New York, NY, USA. She is currently a High School Science Research Teacher and College Counsellor. Her research interests include improving and creating standardized methodologies and analysis tools for hazard modeling.

DIANA CALDERON received the Bachelor of Environmental Science degree and the M.S. degree in geographic information sciences from the City University of New York, Lehman College, New York, NY, USA, in 2019 and 2021, respectively. She is currently a Geographer with the U.S. Census Bureau and a Research Assistant with the Center for International Earth Science Information Network, Palisades, NY, USA.

LAUREN CAREY received the Bachelor of Environmental Science degree in 2020 from the City University of New York, Lehman College, New York, NY, USA, where she is currently working toward the M.S. degree in geographic information science. She is a Regional Science Associate with the NASA SERVIR, Earth System Science Center, University of Alabama in Huntsville, Huntsville, AL, USA.

CHRISTOPHER AIME is currently working toward the M.S. degree in geographic information sciences with the City University of New York, Lehman College, New York, NY, USA. He is also a Research Assistant with the Center for International Earth Science Information Network, Palisades, NY, USA. His research interests include flood risk, wildlife conservation, and remote sensing.

CAROLYNNE HULTQUIST received the B.S. degree in geography and the B.A. degree in international studies from the University of North Carolina at Charlotte, Charlotte, NC, USA, in 2014, and the M.S. and Ph.D. degrees in geography from Pennsylvania State University, State College, PA, USA, in 2016 and 2019, respectively. She is currently a Postdoctoral Research Scientist with the Center for International Earth Science Information Network, Palisades, NY, USA. She develops computational methods for spatio-temporal analysis and modeling of vulnerability to environmental hazards.

GREG YETMAN received the B.A. degree in geography from Saint Mary's University, Halifax, NS, Canada, in 1996 and the M.A. degree in geography from McGill University, Montreal, QC, Canada, in 2000.

He is currently an Associate Director with the Center for International Earth Science Information Network, Palisades, NY, USA. His research interests include application of geographic information technologies in applied research fields, including population geography, natural disasters, and environmental assessment.

ANDREW KRUCZKIEWICZ received the M.A. degree in climate and society from Columbia University, New York, NY, USA, in 2013. He is currently working toward the Ph.D. degree in geo-information science and earth observation with the University of Twente, Enschede, The Netherlands. He is currently a Senior Research Associate with the International Research Institute for Climate and Society, Columbia University. He is a Faculty with the Climate and Society Graduate Program, Columbia's Climate School, New York, NY, USA, and a Science Advisor with the Red Cross Red Crescent Climate Centre, Hague, The Netherlands. He is also Principal Investigator of the NASA GEO Global Flash Flood Risk Project.

YURI GOROKHOVICH received the M.S. degree in engineering and marine geology from Odessa State University, Odessa, Ukraine, in 1983, and the Ph.D. degree in earth and environmental sciences from the City University of New York (CUNY), Lehman College, New York, NY, USA, in 1999. He is currently an Associate Professor with CUNY. He is also a Physical Geologist, who combines geologic and geographic methods, including GIS for the assessment, modeling, and mapping of current and historical natural hazards and disasters.

ROBERT S. CHEN received the B.S. degree in earth and planetary sciences and the two M.S. degrees in earth and planetary sciences and technology and policy from the Massachusetts Institute of Technology, Cambridge, MA, USA, in 1976 and 1982, respectively, and the Ph.D. degree in geography from the University of North Carolina at Chapel Hill, Chapel Hill, NC, USA, in 1987. He is currently the Director of the Center for International Earth Science Information Network, Palisades, NY, USA, a unit of the Columbia Climate School and manages the NASA Socioeconomic Data and Applications Center (SEDAC).